

Preparation and Reactivities of PCP-Type Pincer Complexes of Nickel. Impact of Different Ligand Skeletons and Phosphine Substituents

Annie Castonguay, André L. Beauchamp, and Davit Zargarian*

Département de Chimie, Université de Montréal, Montréal (Québec), Canada H3C 3J7

Received June 10, 2008

Reaction of the diphosphine ligand $i\text{-Pr}_2\text{P}(\text{CH}_2)_5\text{P}(i\text{-Pr})_2$ with NiBr_2 at 110 °C gives a mixture of the 16-membered bimetallic cycle $\{i\text{-Pr}_2\text{P}(\text{CH}_2)_5\text{P}(i\text{-Pr})_2\}_2\text{Ni}_2\text{Br}_4$, **1**, and the pincer-type complex $\{(i\text{-Pr}_2\text{PCH}_2\text{CH}_2)_2\text{CH}\}\text{NiBr}$, **2**; the latter can also be obtained by heating **1** in the presence of 4-(dimethylamino)pyridine or under vacuum. Complex **2** undergoes transmetalation with RMgCl or RLi to give $\{(i\text{-Pr}_2\text{PCH}_2\text{CH}_2)_2\text{CH}\}\text{NiR}$ ($\text{R} = \text{Me}$ (**4**), $\text{C}\equiv\text{CMe}$ (**5**), Ph (**6**), $n\text{-Bu}$ (**7**), and $\text{C}\equiv\text{CPh}$ (**8**)); the phenylacetylide derivative **8** was also obtained from the reaction of $\text{PhC}\equiv\text{CH}$ with **4**, **5**, or **7**. The Ni-Me derivative **4** reacts with PhX ($\text{X} = \text{I, Br, Cl}$) to give the product of C-C coupling reaction (Ph-Me) and the Ni-X analogues of **2**, and tests have shown that **2** is a competent catalytic precursor for the coupling of PhCl and MeMgCl . The available evidence suggests that this catalytic process does not involve Ni^0 intermediates. Indeed, cyclic voltammetry measurements show that **2** can undergo two consecutive oxidations, and attempts to generate isolable high-valent species yielded the five-coordinate, 17-electron Ni^{III} species $\{(i\text{-Pr}_2\text{PCH}_2\text{CH}_2)_2\text{CH}\}\text{NiX}_2$, **9**, from the reaction of **2** with FeX_3 ($\text{X} = \text{Cl, Br}$). Characterization of all new complexes, including X-ray diffraction studies on single crystals of complexes **1–6** and **9**, is described.

Introduction

Many PCP-type pincer complexes¹ are efficient catalysts for a variety of organic transformations.^{2,3} An important advantage of PCP ligands is that they can be modified easily at multiple sites, thus allowing control over the electronic and steric properties of their complexes. For example, it has been demonstrated that the catalytic efficiency of PCP-Pd complexes for the Heck coupling can be improved by changing the nature of the cyclometalated carbon from sp^2 to sp^3 hybridization, incorporating oxygens in the ligand skeleton, varying the phosphorus substituents from $t\text{-Bu}$ to $i\text{-Pr}$, or increasing the size of the metallocycles from five- to six-membered.⁴

Our long-standing interest in organonickel complexes⁵ and the fairly unexplored chemistry of PCP-type pincer complexes of nickel⁶ have prompted us to investigate the preparation of

PCP-Ni complexes and their reactivities. Recent reports have described the results of our initial studies on the synthesis and reactivities of a new series of pincer complexes of nickel based

(5) (a) Gareau, D.; Sui-Seng, C.; Groux, L. F.; Brisse, F.; Zargarian, D. *Organometallics* **2005**, *24*, 4003. (b) Chen, Y.; Sui-Seng, C.; Zargarian, D. *Angew. Chem., Int. Ed.* **2005**, *44*, 7721. (c) Boucher, S.; Zargarian, D. *Can. J. Chem.* **2005**, *84*, 233. (d) Chen, Y.; Sui-Seng, C.; Boucher, S.; Zargarian, D. *Organometallics* **2005**, *24*, 149. (e) Fontaine, F.-G.; Zargarian, D. *J. Am. Chem. Soc.* **2004**, *126*, 8786. (f) Groux, L. F.; Zargarian, D. *Organometallics* **2003**, *22*, 4759. (g) Fontaine, F.-G.; Nguyen, R.-V.; Zargarian, D. *Can. J. Chem.* **2003**, *81*, 1299. (h) Groux, L. F.; Zargarian, D. *Organometallics* **2003**, *22*, 3124. (i) Groux, L. F.; Zargarian, D.; Simon, L. C.; Soares, J. B. P. *J. Mol. Catal. A* **2003**, *19*, 51. (j) Rivera, E.; Wang, R.; Zhu, X. X.; Zargarian, D.; Giasson, R. *J. Mol. Catal. A* **2003**, *325*, 204–205. (k) Zargarian, D. *Coord. Chem. Rev.* **2002**, *157*, 233–234. (l) Wang, R.; Groux, L. F.; Zargarian, D. *Organometallics* **2002**, *21*, 5531. (m) Wang, R.; Groux, L. F.; Zargarian, D. *J. Organomet. Chem.* **2002**, *660*, 98. (n) Fontaine, F.-G.; Zargarian, D. *Organometallics* **2002**, *21*, 401. (o) Dubois, M.-A.; Wang, R.; Zargarian, D.; Tian, J.; Vollmerhaus, R.; Li, Z.; Collins, S. *Organometallics* **2001**, *20*, 663. (p) Groux, L. F.; Zargarian, D. *Organometallics* **2001**, *20*, 3811. (q) Groux, L. F.; Zargarian, D. *Organometallics* **2001**, *20*, 3811. (r) Fontaine, F.-G.; Dubois, M.-A.; Zargarian, D. *Organometallics* **2001**, *20*, 5156. (s) Wang, R.; Bélanger-Gariépy, F.; Zargarian, D. *Organometallics* **1999**, *18*, 5548. (t) Fontaine, F.-G.; Kadkhodazadeh, T.; Zargarian, D. *Chem. Commun.* **1998**, 1253. (u) Vollmerhaus, R.; Bélanger-Gariépy, F.; Zargarian, D. *Organometallics* **1997**, *16*, 4762. (v) Huber, T. A.; Bayraktarian, M.; Dion, S.; Dubuc, I.; Bélanger-Gariépy, F.; Zargarian, D. *Organometallics* **1997**, *16*, 5811. (w) Bayraktarian, M.; Davis, M. J.; Reber, C.; Zargarian, D. *Can. J. Chem.* **1996**, *74*, 2194. (x) Huber, T. A.; Bélanger-Gariépy, F.; Zargarian, D. *Organometallics* **1995**, *14*, 4997.

(6) For examples of PCP complexes of nickel see ref. 1a and: (a) Kennedy, A. R.; Cross, R. J.; Muir, K. W. *Inorg. Chim. Acta* **1995**, *231*, 195. (b) Huck, W. T. S.; Snellink-Ruël, B.; van Veggel, F. C. J. M.; Reinhoudt, D. N. *Organometallics* **1997**, *16*, 4287. (c) Bachechi, F. *Struct. Chem.* **2003**, *14*, 263. (d) Kozhanov, K. A.; Bubnov, M. P.; Cherkasov, V. K.; Fukin, G. K.; Abakumov, G. A. *Chem. Commun.* **2003**, 2610. (e) Câmpora, J.; Palma, P.; del Río, D.; Álvarez, E. *Organometallics* **2004**, *23*, 1652. (f) Câmpora, J.; Palma, P.; del Río, D.; Conejo, M. M.; Álvarez, E. *Organometallics* **2004**, *23*, 5653. (g) van der Boom, M. E.; Liou, S. Y.; Shimon, L. J. W.; Ben-David, Y.; Milstein, D. *Inorg. Chim. Acta* **2004**, *357*, 4015.

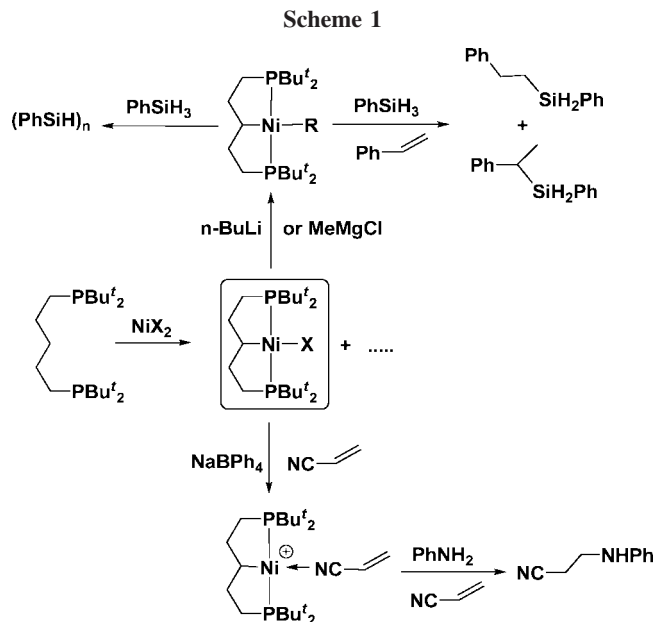
* Corresponding author. E-mail: zargarian.davit@umontreal.ca.

(1) For some of the original reports on PCP-type pincer complexes see: (a) Moulton, C. J.; Shaw, B. L. *Dalton Trans.* **1976**, 1020. (b) Al-Salem, N. A.; Empsall, H. D.; Markham, R.; Shaw, B. L.; Weeks, B. *Dalton Trans.* **1979**, 1972. (c) Al-Salem, N. A.; McDonald, W. S.; Markham, R.; Norton, M. C.; Shaw, B. L. *Dalton Trans.* **1980**, 59. (d) Crocker, C.; Errington, R. J.; Markham, R.; Moulton, C. J.; Odell, K. J.; Shaw, B. L. *J. Am. Chem. Soc.* **1980**, *102*, 4373. (e) Crocker, C.; Errington, R. J.; Markham, R.; Moulton, C. J.; Shaw, B. L. *Dalton Trans.* **1982**, 387. (f) Crocker, C.; Empsall, H. D.; Errington, R. J.; Hyde, E. M.; McDonald, W. S.; Markham, R.; Norton, M. C.; Shaw, B. L.; Weeks, B. *Dalton Trans.* **1982**, 1217. (g) Briggs, J. R.; Constable, A. G.; McDonald, W. S.; Shaw, B. L. *Dalton Trans.* **1982**, 1225.

(2) (a) Albrecht, M.; van Koten, G. *Angew. Chem., Int. Ed.* **2001**, *40*, 3750. (b) van der Boom, M. E.; Milstein, D. *Chem. Rev.* **2003**, *103*, 1759.

(3) Singleton, J. T. *Tetrahedron* **2003**, *59*, 1837.

(4) (a) Sjövall, S.; Wendt, O. F.; Andersson, C. *J. Chem. Soc., Dalton Trans.* **2002**, 1396. (b) Ohff, M.; Ohff, A.; van der Boom, M. E.; Milstein, D. *J. Am. Chem. Soc.* **1997**, *119*, 11687. (c) Miyazaki, F.; Yamaguchi, K.; Shibasaki, M. *Tetrahedron Lett.* **1999**, *40*, 7379. (d) Naghipour, A.; Sabounchei, S. J.; Morales-Morales, D.; Canseco-González, D.; Jensen, C. M. *Polyhedron* **2007**, *26*, 1445.



on the PCP-type ligands 1,3-(CH₂CH₂PPh₂)₂-indenyl⁷ and *t*-Bu₂P(CH₂)₅P(*t*-Bu)₂ (PC_{sp3}P^{*t*-Bu}).^{8,9} We found, for example, that reacting the latter ligand with NiX₂ (X = Cl, Br, I) gives a mixture of the desired pincer-type complex {(*t*-Bu₂PCH₂-CH₂)₂CH}NiX along with paramagnetic species believed to be zwitterionic and dianionic tetrahedral complexes featuring the unmetalated pincer ligand (Scheme 1). The Ni(PC_{sp3}P^{*t*-Bu})X complexes (X = H, Me) promote the dehydrogenative oligomerization of PhSiH₃ and its addition to styrene, whereas their cationic NCR adducts (R = Me, CH=CH₂) promote the hydroamination of acrylonitrile with aniline (Scheme 1).

Subsequent studies focused on modifying the PC_{sp3}P ligand framework in order to evaluate the influence of ligand architecture on the reactivities of the resulting complexes. Thus, we found that some Ni pincer complexes based on the diphosphinito-type ligands (*i*-Pr₂POCH₂)₂CH₂ (POC_{sp3}OP^{*i*-Pr}) or 1,3-(*i*-Pr₂PO)₂C₆H₄ (POC_{sp2}OP^{*i*-Pr}) are efficient catalysts for the hydroamination of acrylonitrile derivatives and the Kharasch addition of CCl₄ to olefins.¹⁰

As an extension of our initial studies, we have investigated the impact of phosphine substituents on the syntheses of pincer-type compounds and their reactivities. The present report describes the synthesis and reactivities of new Ni complexes based on the diphosphine ligand *i*-Pr₂P(CH₂)₅P(*i*-Pr)₂ (PC_{sp3}-P^{*i*-Pr}), including the pincer-type Ni^{II} and Ni^{III} compounds (PC_{sp3}-P^{*i*-Pr})NiX (X = Br, Me, C≡CMe, Ph, *n*-Bu, and C≡CPh) and (PC_{sp3}-P^{*i*-Pr})NiX₂ (X = Br, Cl). Also reported are the synthesis and solid state structure of {*i*-Pr₂P(CH₂)₅P(*i*-Pr)₂}₂Ni₂Br₄, a dimeric species featuring the nonmetalated ligand.

Results and Discussion

Synthesis of {*i*-Pr₂P(CH₂)₅P(*i*-Pr)₂}₂Ni₂Br₄, **1, and {(*i*-Pr₂PCH₂CH₂)₂CH}NiBr, **2**.** Mixing the diphosphine ligand PC_{sp3}P^{*i*-Pr} with NiBr₂ for 2 h at 80 °C gave 93% yield of a

purple solid that was identified as the 16-membered bimetal-lacycle complex **1** (Scheme 2). Increasing the reaction temperature to 110 °C afforded, after 12 h, a mixture of products consisting of **1** as the major component (>80%) along with a small amount (<10%) of a golden-brown solid identified as the pincer-type complex **2** (Scheme 2). Carrying out the latter reaction in more dilute conditions did not lead to a better yield of the target complex **2**, but the presence of 1 equiv of 4-(dimethylamino)pyridine (DMAP) in the reaction mixture gave a 37% yield of complex **2** (Scheme 2). Interestingly, heating a 1:2 mixture of pure **1** and DMAP gives **2** with a similar yield, which implies that **1** might be an intermediate in the formation of **2**. Finally, a small amount of **2** was also obtained (along with some free ligand) when a solid sample of complex **1** was heated to 200–220 °C under reduced pressure for a few hours; a similar transformation has been reported for {*t*-Bu₂P(CH₂)₅-P(*t*-Bu)₂}₂Pd₂Cl₄.^{1b,11}

Complexes **1** and **2** can be handled in air, both in the solid state and in solution, without noticeable decomposition even after weeks. The NMR spectra of these complexes were quite different from one another, showing that complex **1** adopts a fluxional structure in solution, whereas **2** displays spectral patterns typical of pincer complexes. For instance, the room-temperature ³¹P{¹H} NMR spectrum of **1** showed no signal at all, while the room-temperature ¹H and ¹³C{¹H} NMR spectra displayed broad, featureless signals; interestingly, the ¹³C{¹H} chemical shifts were quite similar for **1** and the uncoordinated ligand. Lowering the probe temperature to -15 °C led to the emergence of a broad ³¹P{¹H} signal (17 ppm), but this and the ¹H and ¹³C{¹H} signals did not sharpen appreciably even at -50 °C, thus providing little structural information for complex **1**.

In contrast, NMR spectroscopy was very helpful in establishing the solution structure of complex **2**, as follows. The equivalence of the phosphorus nuclei was confirmed by the presence of one singlet resonance (67.4 ppm) in the room-temperature ³¹P{¹H} NMR spectrum of **2**, while the *trans* disposition of the phosphorus atoms in this complex was suggested by the presence of virtual triplets in the ¹H and ¹³C{¹H} NMR spectra for the methyl protons and carbons of the isopropyl groups. The ¹³C{¹H} NMR spectrum also displayed virtual triplets for the α- and β- carbons of the alkyl chain of the ligand, and the cyclometalation of the central carbon atom was confirmed by the presence of a downfield-shifted triplet signal (52 ppm, ²J_{PC} = 9 Hz; free ligand: 34 ppm).

The solid state structures of **1** and **2** were established by X-ray analyses of single crystals of these compounds.¹² The crystal data and collection details are listed in Table 1, whereas ORTEP views are shown in Figures 1 and 2. The nickel center in **1** adopts a slightly distorted square-planar geometry, the P–Ni–P and Br–Ni–Br angles varying between ~166° and ~173°. The Ni–Br bond lengths (2.30–2.32 Å) are within the expected range for *trans*-NiP₂Br₂ arrangements (ca. 2.30),¹³ whereas the Ni–P bond lengths (2.25–2.27 Å) are similar to those of the analogous species {*i*-Pr₂P(CH₂)₅P(*i*-Pr)₂}₂Ni₂Cl₄ (2.24–2.26 Å).¹² The size of the macrocycle can be estimated from the distances between P1 and P3 (9.6 Å), P2 and P4 (9.1 Å), C3 and C8 (6.0 Å), and Ni1 and Ni2 (8.4 Å).

(7) Groux, L. F.; Bélanger-Garlépy, F.; Zargarian, D. *Can. J. Chem.* **2005**, *83*, 634.

(8) Castonguay, A.; Sui-Seng, C.; Zargarian, D.; Beauchamp, A. L. *Organometallics* **2006**, *25*, 02.

(9) Sui-Seng, C.; Castonguay, A.; Chen, Y.; Gareau, D.; Groux, L. F.; Zargarian, D. *Top. Catal.* **2006**, *37*, 81.

(10) (a) Pandarus, V.; Zargarian, D. *Chem. Commun.* **2007**, 978. (b) Pandarus, V.; Zargarian, D. *Organometallics* **2007**, *26*, 4321.

(11) Seligson, A. L.; Troglér, W. C. *Organometallics* **1993**, *12*, 738.

(12) The preparation and the X-ray analysis of a single crystal of {*i*-Pr₂P(CH₂)₅P(*i*-Pr)₂}₂Ni₂Cl₄, the Cl analogue of **1**, have been reported recently. Castonguay, A.; Beauchamp, A. L.; Zargarian, D. *Acta Crystallogr.* **2007**, *E63*, m196.

(13) Cambridge Structural Database search (Version 5.28 with updates up to November 2006): Allen, F. H. *Acta Crystallogr.* **2002**, *B58*, 380.

Scheme 2

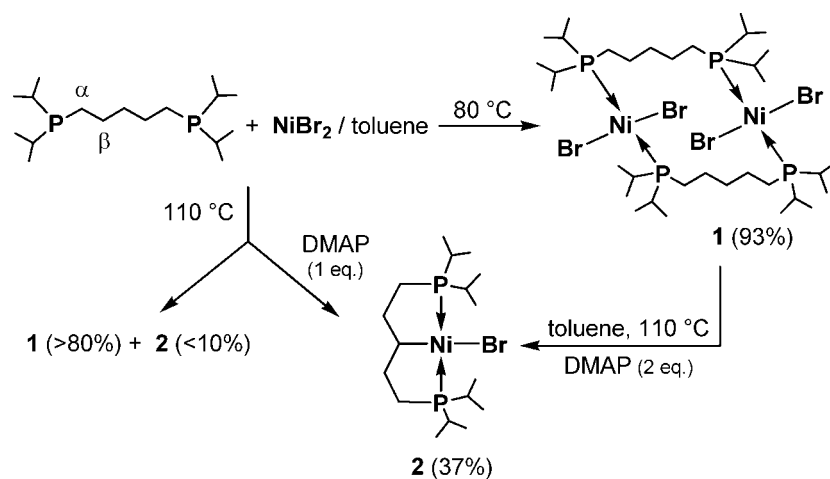


Table 1. Crystal Data Collection and Refinement Parameters for Complexes 1–6 and 9

	1	2	3	4	5	6	9b
chemical formula	C ₃₄ H ₇₆ Br ₄ Ni ₂ P ₄	C ₁₇ H ₃₇ BrNiP ₂	C ₂₀ H ₃₅ BrNiP ₂	C ₁₈ H ₄₀ NiP ₂	C ₂₀ H ₄₀ NiP ₂	C ₂₃ H ₄₂ NiP ₂	C ₁₇ H ₃₇ Br ₂ NiP ₂
fw	1045.89	442.03	476.04	377.15	401.17	439.22	521.92
<i>T</i> (K)	220(2)	100(2)	150(2)	100(2)	220(2)	220(2)	150(2)
wavelength (Å)	1.54178	1.54178	1.54178	1.54178	1.54178	1.54178	1.54178
space group	<i>Pbca</i>	<i>P2₁/n</i>	<i>R$\bar{3}c$</i>	<i>P2₁/c</i>	<i>P2₁/n</i>	<i>P2₁/n</i>	<i>Pbca</i>
<i>a</i> (Å)	23.6525 (13)	8.4858(2)	25.2547(3)	14.2542(6)	10.8603(6)	10.1898(9)	14.0098(16)
<i>b</i> (Å)	14.4554 (9)	11.8590(3)	25.2547(3)	13.7514(6)	14.5551(9)	12.5298(12)	16.2434(18)
<i>c</i> (Å)	27.6110 (16)	20.8903(5)	20.6154(5)	10.5561(4)	14.1473(8)	19.3011(16)	38.914(4)
α (deg)	90	90	90	90	90	90	90
β (deg)	90	90.7960(10)	90	95.091(2)	92.175(2)	97.936(4)	90
γ (deg)	90	90	120	90	90	90	90
<i>Z</i>	8	4	18	4	4	4	16
<i>V</i> (Å ³)	9440.4 (10)	2102.05(9)	11386.9(3)	2060.99(15)	2234.7(2)	2440.7(4)	8855.5(17)
ρ_{calcd} (g cm ⁻³)	1.472	1.397	1.250	1.215	1.192	1.195	1.566
μ (cm ⁻¹)	63.85	49.23	41.32	27.49	25.68	23.95	68.07
θ range (deg)	3.20–73.04	4.23–68.81	3.50–68.45	3.11–68.87	4.36–72.03	4.22–72.00	2.27–65.85
<i>R</i> 1 ^a [<i>I</i> > 2 σ (<i>I</i>)]	0.0615	0.0322	0.0436	0.0395	0.0410	0.0486	0.0328
<i>wR</i> 2 ^b [<i>I</i> > 2 σ (<i>I</i>)]	0.1303	0.0811	0.1517	0.1019	0.1118	0.1264	0.0757
<i>R</i> 1 [all data]	0.0704	0.0382	0.0517	0.0468	0.0427	0.0549	0.0520
<i>wR</i> 2 [all data]	0.1360	0.0838	0.1518	0.1068	0.1134	0.1317	0.0812
GOF	1.079	1.021	1.186	1.003	1.084	1.023	0.963

^a $R1 = \sum(|F_o| - |F_c|) / \sum |F_o|$. ^b $wR2 = \{ \sum [w(F_o^2 - F_c^2)^2] / \sum [w(F_o^2)^2] \}^{1/2}$.

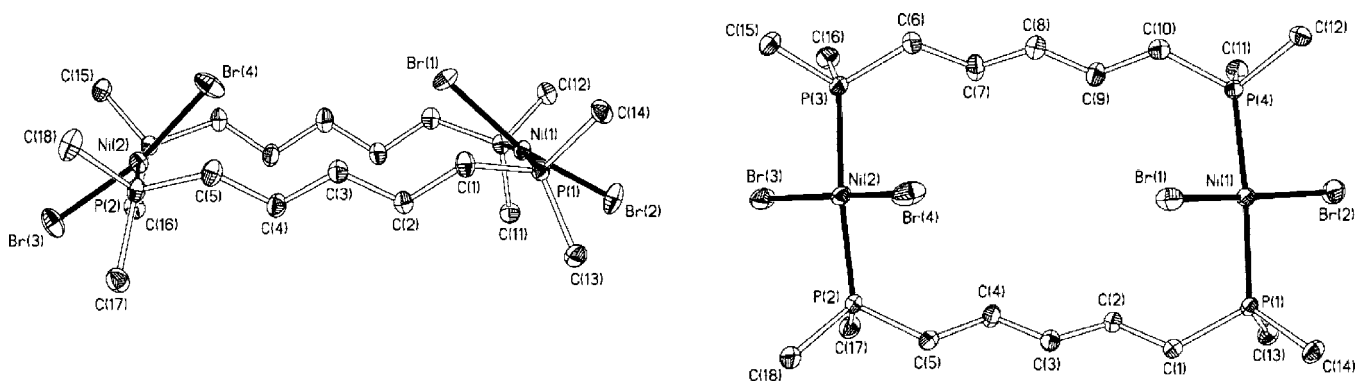


Figure 1. ORTEP diagrams for complex 1. Thermal ellipsoids are shown at the 30% probability level. Hydrogens and *i*-Pr methyl carbons are omitted for clarity. Selected bond distances (Å) and angles (deg): Ni(1)–P(1) = 2.2494(10), Ni(1)–P(4) = 2.2466(10), Ni(2)–P(2) = 2.2680(10), Ni(2)–P(3) = 2.2704(10), Ni(1)–Br(1) = 2.3038(6), Ni(1)–Br(2) = 2.3125(7), Ni(2)–Br(3) = 2.3244(7), Ni(2)–Br(4) = 2.3013(7), P(1)–Ni(1)–P(4) = 171.85(4), P(2)–Ni(2)–P(3) = 173.36(4), Br(1)–Ni(1)–Br(2) = 165.99(3), Br(3)–Ni(2)–Br(4) = 167.83(4).

The Ni center in **2** adopts a square-planar geometry wherein all structural parameters (Table 2) are in the expected range. This solid state structure confirms the metalation of the ligand as inferred from the solution NMR spectra. Comparison of Ni–ligand bond lengths in **2** and its *t*-Bu analogue $\{(t\text{-Bu})_2\text{PCH}_2\text{-CH}_2\text{CH}_2\text{CH}\}\text{NiBr}^{\delta}$ (Table 2) shows that the main structural impact

brought about by the change of the phosphorus substituents is on the Ni–P bond distances, which are significantly shorter in complex **2** (ca. 2.18 vs 2.21 Å). We infer that the greater steric bulk of the *t*-Bu groups must prevent the phosphine moieties from approaching the metal center sufficiently to allow optimal orbital overlap.

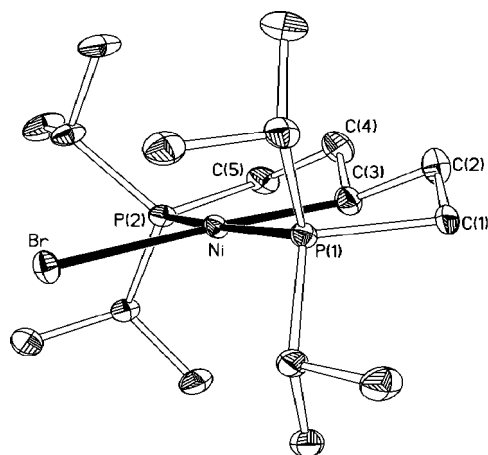


Figure 2. ORTEP diagram for complex **2**. Thermal ellipsoids are shown at the 30% probability level. Hydrogens are omitted for clarity.

In order to assess the structural differences in PCP-type pincer complexes featuring aliphatic versus aromatic linkers, we have prepared complex $\{(i\text{-Pr})_2\text{PCH}_2)_2\text{C}_6\text{H}_3\}\text{NiBr}$, **3**, the previously reported¹⁴ $\text{PC}_{\text{sp}^2}\text{P}$ analogue of **2**, and examined its solid state structure. ORTEP views of **3** are shown in Figure 3, and crystal data are listed in Table 1. We found that the Ni–P and the Ni–Br bond lengths are approximately the same in both complexes, but that the Ni–C bond is shorter in **3** (1.92 vs 1.98 Å), as expected for a M–C bond distance with greater s character (Table 2).

Reactivities of 2. Our interest in exploring the potential of PCP–Ni compounds as promoters of carbon–carbon bond formation reactions led us to prepare organonickel derivatives of complex **2** and compare their stabilities and reactivities as a function of phosphine substituents. We found that **2** reacts with MeMgCl or $\text{MeC}\equiv\text{CMgBr}$ at room temperature to give the Ni–Me (**4**, ca. 71%) and Ni–C \equiv CMe (**5**, 79%) derivatives, respectively, whereas the reaction with PhMgBr required refluxing in THF for 1 h to give the Ni–Ph derivative (**6**, ca. 62% yield, Scheme 3). By comparison, preparation of the analogous Ni–Me derivative based on the $\text{PC}_{\text{sp}^3}\text{P}^{i\text{-Bu}}$ ligand was less facile, requiring heating for at least 1 h for total conversion,⁸ whereas the Ni–Ph derivative could not be prepared with this ligand even after extended heating. Phosphine substituents also influence the stability of the alkyl derivatives toward β -hydrogen elimination. Thus, solutions of the Ni–Bu derivative **7** obtained from the reaction of **2** with $n\text{-BuLi}$ are stable for hours at room temperature (Scheme 3), whereas under the same conditions the analogous complex $(\text{PC}_{\text{sp}^3}\text{P}^{i\text{-Bu}})\text{Ni-Bu}$ undergoes β -hydrogen elimination within a few minutes to give the corresponding hydride complex (and a considerable amount of free ligand); this difference of reactivity likely arises from the steric blocking of the $d_{z^2}\text{-}p_z$ hybrid orbital by the $(i\text{-Pr})_2\text{P}$ groups that are at a closer proximity to the Ni center in comparison to their $(t\text{-Bu})_2\text{P}$ analogues.⁸

Spectroscopic characterization of complexes **4–7** was relatively straightforward. The appearance of a singlet resonance in the $^31\text{P}\{^1\text{H}\}$ NMR spectrum of each derivative (71.4, 76.1, 68.1, and 68.1 ppm for **4**, **5**, **6** and **7**, respectively) demonstrated the equivalence of the phosphine moieties, while the maintenance of their *trans* arrangement was reflected in the presence of virtual triplets in their respective ^1H and $^{13}\text{C}\{^1\text{H}\}$ NMR

spectra. The metalated nature of the central CH group was evident from a slightly downfield-shifted triplet (56–59 ppm, $^2J_{\text{PC}} \sim 9\text{--}10$ Hz; free ligand: 34 ppm) in the $^{13}\text{C}\{^1\text{H}\}$ NMR spectrum for each of these complexes.

The Ni–Me moiety in complex **4** was represented by high-field triplet resonances in its ^1H (–0.50 ppm, $^3J_{\text{P-H}} = 7.7$ Hz) and $^{13}\text{C}\{^1\text{H}\}$ (–18.64 ppm, $^2J_{\text{PC}} = 19.9$ Hz) NMR spectra. The $^{13}\text{C}\{^1\text{H}\}$ NMR spectrum of complex **5** exhibited three resonances for the propynyl moiety: a triplet at 98.44 ppm ($^2J_{\text{PC}} = 30.8$ Hz, Ni–C \equiv CCH₃), a singlet at 115.74 ppm (Ni–C \equiv CCH₃), and a singlet at 7.61 ppm (Ni–C \equiv CCH₃). The ^1H NMR spectrum of this complex showed a singlet at 2.13 ppm corresponding to the methyl protons of the propynyl moiety, while the IR spectrum showed a sharp band at 2100 cm^{-1} , which was assigned to $\nu_{\text{C}=\text{C}}$. The Ni–Ph moiety of complex **6** was identified by the appearance in the ^1H and $^{13}\text{C}\{^1\text{H}\}$ NMR spectra of signals corresponding to the five nonequivalent aromatic protons and carbon nuclei, in addition to a low-field triplet resonance assigned to the *ipso*-C (168.77 ppm, $^2J_{\text{PC}} = 24.0$ Hz). The nonequivalence of the carbons and protons of the Ni–Ph moiety implies that the phenyl ring does not undergo rapid rotation in solution and does not lie in the coordination plane of the molecule; the solid state structure of this complex confirms a noncoplanar conformation for the Ph ring (*vide infra*). The $^{13}\text{C}\{^1\text{H}\}$ NMR spectrum of complex **7** showed two triplet resonances assigned to Ni–CH₂ (0.51 ppm, $^2J_{\text{PC}} = 19.0$ Hz) and Ni–CH₂CH₂ (36.41 ppm, $^3J_{\text{PC}} = 2.3$ Hz) and two singlets assigned to Ni–CH₂CH₂CH₂ (31.02 ppm) and Ni–CH₂CH₂CH₂CH₃ (14.46 ppm), while its ^1H NMR spectrum displayed a multiplet at 0.50 ppm, which was assigned to NiCH₂.

The solid state structures of **4–6** were studied by X-ray analyses performed on single crystals of these compounds. The ORTEP views of the three complexes are shown in Figure 4, the crystal data and collection details are listed in Table 1, and selected bond distances and angles are given in Table 2. The nickel center maintains a distorted square-planar geometry in all three structures. In comparison to the corresponding distances in the Ni–Br derivative **2**, the Ni–P bonds are shorter ($\sim 2.14\text{--}2.16$ vs 2.18 Å) and the Ni–C(3) bonds longer ($\sim 1.99\text{--}2.00$ vs 1.98 Å) in **4–6**. The mean plane defined by the phenyl ring in complex **6** makes an angle of ca. 75° with the NiP₂C plane.¹⁵ The alkynyl moiety in **5** is slightly tilted at C10 (Ni–C(10)–C(11) $\sim 172^\circ$) but is otherwise linear (C(10)–C(11)–C(12) $\sim 176^\circ$).

Inspection of the Ni–R bond lengths found in these pincer species shows their anticipated dependence on the hybridization of the carbon atom in each case (i.e., Ni–C_{sp} < Ni–C_{sp2} < Ni–C_{sp3}). We note also that these Ni–R bonds are significantly longer than the mean value for the corresponding bond distances found in the literature:¹³ 2.02 Å in **4** vs 1.96 Å for other Ni–Me distances; 1.91 Å in **5** vs 1.87 Å for other Ni–C \equiv CR distances; ¹⁶ 1.94 Å in **6** vs 1.90 Å for other Ni–Ph distances. The longer Ni–C bonds in these complexes can be explained by the high *trans* influence exerted by the sp³-hybridized central carbon atom of the $\text{PC}_{\text{sp}^3}\text{P}^{i\text{-Pr}}$ ligand.

Reaction of Phenylacetylene with $(\text{PC}_{\text{sp}^3}\text{P}^{i\text{-Pr}})\text{Ni-R}$. The relative strengths of M–C bonds usually follow the order M–C_{sp} > M–C_{sp2} > M–C_{sp3} such that converting M–C_{sp3}

(15) Presumably, this orientation avoids a repulsive interaction between the filled $d_{z^2}\text{-}p_z$ hybrid orbital and the symmetry-related MO on the Ph moiety.

(16) Since complex **5** is, to our knowledge, the first reported molecular structure of a Ni–C \equiv CMe complex where the propynyl ligand is not bridged with another metal, we compared the Ni–C_{sp} bond distance in **5** to the mean of all the Ni–alkynyl bond lengths reported in the literature.

Table 2. Selected Bond Distances (Å) and Angles (deg) for Complexes 2–6

	(PC _{sp3} P ^{i-Pr})NiBr (2)	(PC _{sp3} P ^{i-Bu})NiBr ⁸	(PC _{sp2} P ^{i-Pr})NiBr (3)	(PC _{sp3} P ^{i-Pr})NiMe (4)	(PC _{sp3} P ^{i-Pr})NiCCMe (5)	(PC _{sp3} P ^{i-Pr})NiPh (6)
Ni–C(3)	1.9820(30)	1.9710(40)	1.9180(30)	2.0040(20)	1.9917(17)	2.0060(20)
Ni–P(1)	2.1801(7)	2.2182(12)	2.1645(6)	2.1535(6)	2.1491(5)	2.1479(6)
Ni–P(2)	2.1794(7)	2.2123(12)	2.1645(6) ^a	2.1381(6)	2.1604(5)	2.1455(6)
Ni–X	2.3712(5)	2.3866(7)	2.3443(6)	2.0160(20)	1.9140(20)	1.9440(20)
C(3)–Ni–X	177.22(8)	169.89(13)	180.00(17)	172.81(9)	174.28(8)	177.46(10)
P(1)–Ni–P(2)	171.13(3)	170.16(5)	170.60(4) ^a	170.05(3)	170.57(2)	170.24(2)
P(1)–Ni–X	94.76(2)	94.48(3)	94.70(2)	94.93(6)	91.74(5)	94.27(6)
P(2)–Ni–X	94.09(2)	95.00(4)	94.70(2) ^a	94.74(6)	97.64(5)	95.46(6)
P(1)–Ni–C(3)	86.08(8)	85.90(13)	85.30(2)	84.80(6)	85.42(5)	84.57(7)
P(2)–Ni–C(3)	85.05(8)	85.22(13)	85.30(2) ^a	85.91(6)	85.15(5)	85.68(7)

^a Symmetry transformation used to generate equivalent atoms: $y + 1/3, x - 1/3, -z + 1/6$.

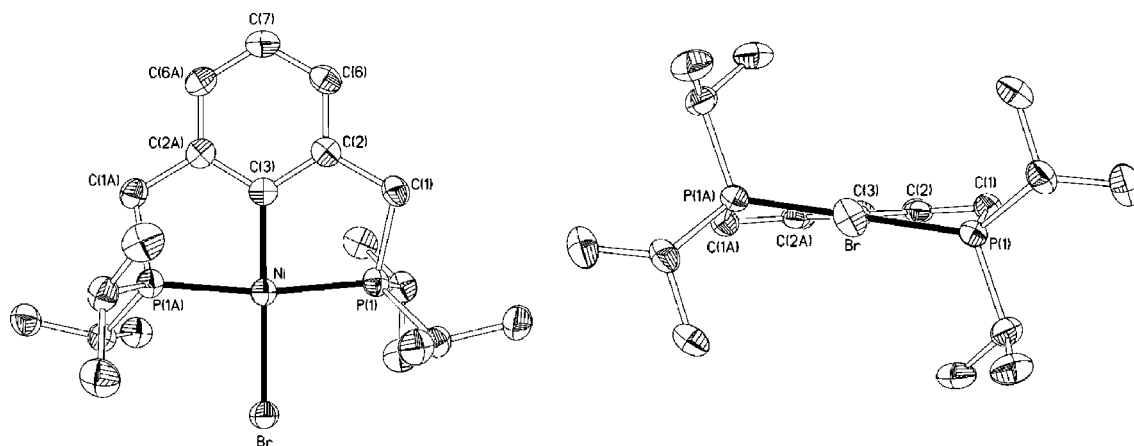
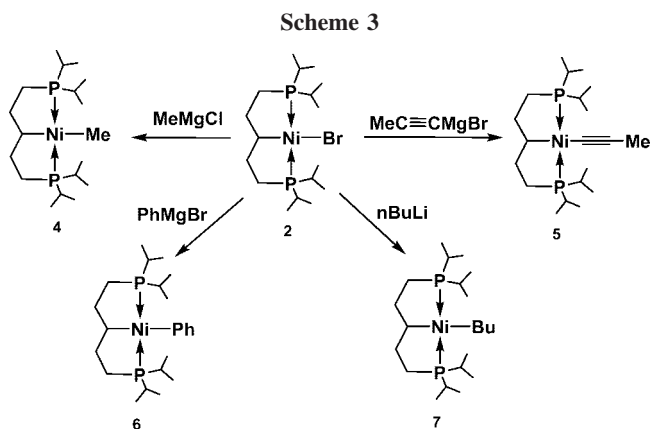


Figure 3. ORTEP diagrams for complex 3. Thermal ellipsoids are shown at the 30% probability level. Hydrogens are omitted for clarity.



bonds to the stronger M–C_{sp2} or M–C_{sp} bonds should be thermodynamically favorable. Accordingly, we have found that the Ni–Me complex **4** and the Ni–Bu **7** react with PhC≡CH at room temperature to give the corresponding Ni–C≡CPh derivative **8** (Scheme 4). The corresponding reaction also proceeds with the Ni–C≡CMe derivative **5**, but this reaction required heating to go to completion, whereas the Ni–Ph complex **6** did not lead to **8** even with extended heating in the presence of PhC≡CH.¹⁷ The Ni–C≡CPh complex **8**, which was also prepared by reacting **2** with LiC≡CPh (Scheme 4), was obtained as an oily solid that could not be isolated in pure form, but its identity has been confirmed by NMR spectroscopy.

The conversion of **4**, **5**, and **7** to **8** raises the question of whether these reactions proceed by a sequence of oxidative

addition and reductive elimination or via a concerted process involving σ -bond metathesis. NMR monitoring of the reaction of **5** with PhC≡CH did not reveal any intermediates, precluding any direct evidence in favor of a mechanism involving discrete addition/elimination steps. In an effort to determine whether or not the “protonolysis” of the Ni–R moiety by PhC≡CH involves oxidative addition of the C_{sp}–H bond, we investigated the kinetic isotope effects (KIE) for the reaction of **5** with PhC≡CH/D. These studies have shown that the KIE values, which cover a relatively wide range (0.1–12), are strongly dependent on solvent polarity and reaction temperature; unfortunately, however, the results were not reproducible, precluding any reliable conclusions at this point on the question of whether these reactions are concerted processes or involve discrete addition/elimination steps.

Kumada Coupling. Recent reports have shown that the coupling of Grignard reagents and aryl halides, first reported independently by the groups of Kumada¹⁸ and Corriu,¹⁹ can be efficiently catalyzed by PNP-, PNN-, and NNN-type pincer complexes of Ni^{II}.²⁰ Since Grignard reagents readily transform our Ni–Br complex **2** to the corresponding Ni–R derivatives, we set out to test if (PC_{sp3}P^{i-Pr})NiR would react with phenyl halides to give coupling products. Heating the Ni–Me complex **4** with excess PhX (X = I, Br, Cl; C₆D₆ solutions at 60 °C) produced toluene, as detected by GC/MS; analysis of the final mixtures by ³¹P{¹H} NMR spectroscopy showed the conversion of **4** to the Ni–X derivatives.²¹ The observed degrees of conversion indicated that the coupling reaction is more facile

(18) Tamao, K.; Sumitani, K.; Kumada, M. *J. Am. Chem. Soc.* **1972**, *94*, 4374.

(19) Corriu, R. J. P.; Masse, J. P. *Chem. Commun.* **1972**, 144.

(20) (a) Wang, Z.-X.; Wang, L. *Chem. Commun.* **2007**, 2423. (b) Liang, L.-C.; Chien, P.-S.; Lin, J.-M.; Huang, M.-H.; Huang, Y.-L.; Liao, J.-H. *Organometallics* **2006**, *25*, 1399.

(17) In the case of the reaction involving Ni–Ph (**6**) or Ni–Bu (**7**), some uncharacterized minor products were noted by ³¹P{¹H} NMR spectroscopy.

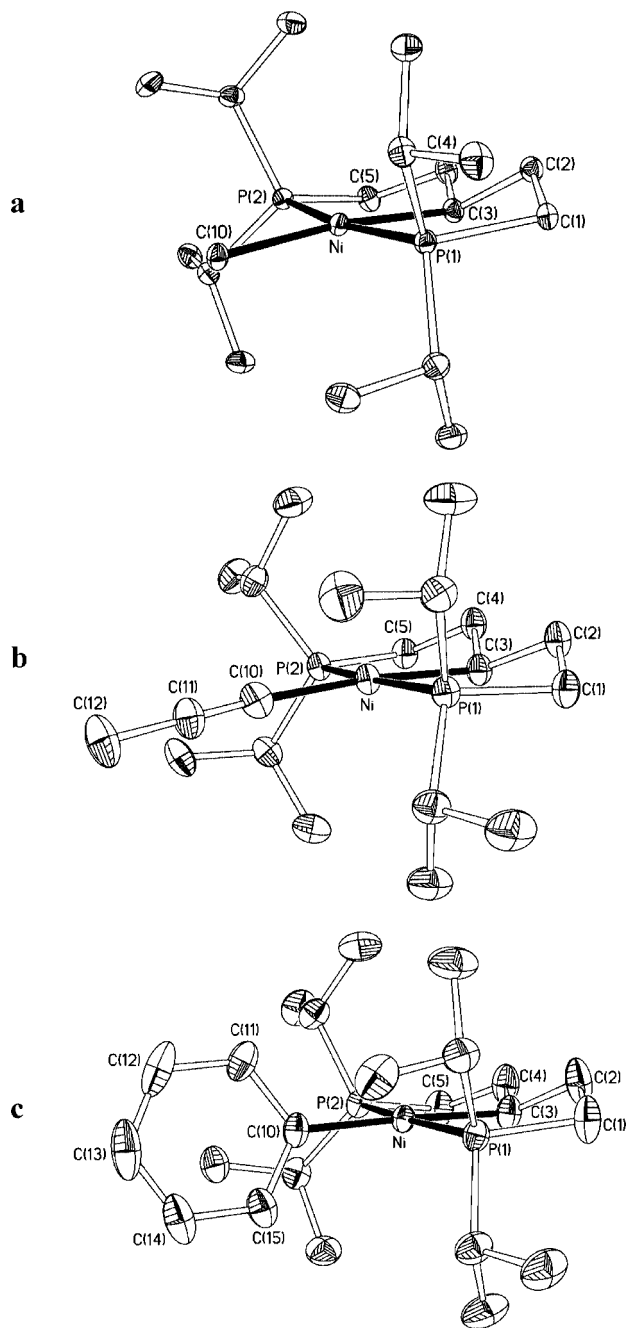
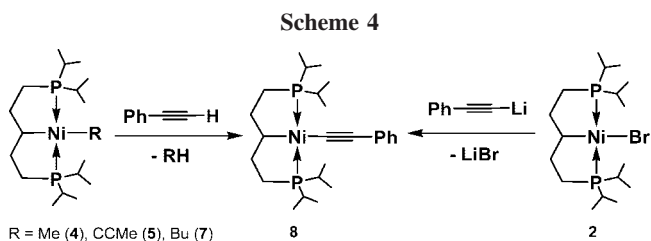


Figure 4. ORTEP diagram for complexes **4** (a), **5** (b), and **6** (c). Thermal ellipsoids are shown at the 30% probability level. Hydrogens are omitted for clarity.



in the order $\text{PhI} > \text{PhBr} > \text{PhCl}$; nevertheless, refluxing **4** in neat PhCl for 1 h gave complete conversion to the Ni–Cl derivative and toluene (Scheme 5).

Having established that **4** can promote the C–C bond formation reaction, we examined the competence of complex **2** for catalyzing the Kumada–Corriu coupling reaction between

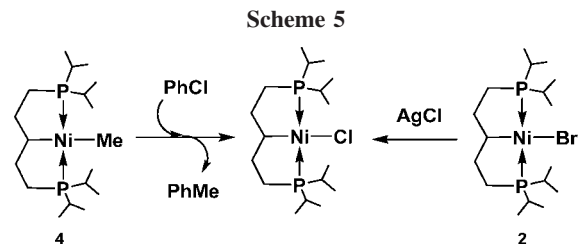


Table 3. Kumada Coupling Reactions Catalyzed by $(\text{PCP})\text{NiX}^a$

MeMgCl + Ph–Cl		catalyst	Ph–Me + Ph–Ph	
		THF reflux 20 h	yield (%) ^b	
run	catalyst (mol %)		Ph–Me	Ph–Ph
1	2 (2.0)		67	2
2	2 (1.0)		57	3
3	2 (0.5)		42	4
4	$\text{Ni}(\text{PC}_{\text{sp}^3}\text{P}^{\text{f-Bu}})\text{Br}$ (1.0)		34	3
5	3 (1.0)		1	0

^a Reaction conditions: 2 mmol of chlorobenzene, 3 mmol of MeMgCl, 0.5 mmol of *p*-xylene (used as an internal standard), 1.0 mL of THF (conditions not optimized). ^b Yields were determined by GC/MS and are the average of three runs.

MeMgCl and chlorobenzene. The organic products of these reactions were identified by GC/MS analyses, and the catalysis yields were determined from independently prepared calibration curves using authentic samples. As can be seen from Table 3, **2** catalyzes the desired heterocoupling reaction in refluxing THF with up to 84 turnovers; minor amounts of the homocoupling product are also produced (runs 1–3). Preliminary results have also shown that under similar conditions **2** also couples chlorobenzene and *n*-BuMgCl, an alkyl chain bearing hydrogens in the β -position.

Tests showed that the catalysis proceeds less efficiently with the closely related species $(\text{PC}_{\text{sp}^3}\text{P}^{\text{f-Bu}})\text{NiBr}$ ⁸ (run 4), whereas complex **3** is nearly inactive for this reaction (run 5). Combining these results with our observations from cyclic voltammetry measurements (*vide infra*) suggests a direct correlation between the catalytic efficiency of these PCP systems and the respective electron richness of their Ni centers ($\mathbf{2} > (\text{PC}_{\text{sp}^3}\text{P}^{\text{f-Bu}})\text{NiBr} > \mathbf{3}$).

The coupling reaction catalyzed by **2** was monitored by ³¹P{¹H} NMR spectroscopy in order to gain some insight into the mechanism of this process in our system. This experiment showed that the only P-containing (and diamagnetic) species present during the course of the catalysis is the Ni–Me complex **4** (a singlet observed at 71.4 ppm), which implies that this species is the resting state of the catalysis. Furthermore, this

(21) The spectral assignments for Ni–Cl and Ni–I derivatives were confirmed against the independently prepared samples from the reaction of **2** with AgCl and anhydrous NiI₂ with *i*-Pr₂P(CH₂)₃P(*i*-Pr)₂, respectively. Selected spectral data for $(\text{PC}_{\text{sp}^3}\text{P}^{\text{f-Bu}})\text{NiCl}$: ¹³C{¹H} NMR (C₆D₆): 17.57 (s, CH(CH₃)₂, 2C), 18.63 (s, CH(CH₃)₂, 2C), 19.28 (s, CH(CH₃)₂, 2C), 19.66 (s, CH(CH₃)₂, 2C), 21.78 (vt, ^νJ_{PC} = 10.7 Hz, CH₂P, 2C), 22.89 (vt, ^νJ_{PC} = 10.3 Hz, CH(CH₃)₂, 2C), 24.98 (vt, ^νJ_{PC} = 9.3 Hz, CH(CH₃)₂, 2C), 39.01 (vt, ^νJ_{PC} = 9.3 Hz, CH₂CH₂P, 2C), 48.74 (t, ²J_{PC} = 9.7 Hz, CHNi, 1C). ³¹P{¹H} NMR (C₆D₆): 66.5. Selected spectral data for $(\text{PC}_{\text{sp}^3}\text{P}^{\text{f-Bu}})\text{NiI}$: ¹³C{¹H} NMR (C₆D₆): 17.70 (s, CH(CH₃)₂, 2C), 18.68 (s, CH(CH₃)₂, 2C), 19.54 (vt, ^νJ_{PC} = 2.4 Hz, CH(CH₃)₂, 2C), 20.41 (s, CH(CH₃)₂, 2C), 22.69 (vt, ^νJ_{PC} = 10.3 Hz, CH₂P, 2C), 24.44 (vt, ^νJ_{PC} = 11.4 Hz, CH(CH₃)₂, 2C), 26.35 (vt, ^νJ_{PC} = 10.3 Hz, CH(CH₃)₂, 2C), 38.81 (vt, ^νJ_{PC} = 10.0 Hz, CH₂CH₂P, 2C), 57.97 (t, ²J_{PC} = 8.3 Hz, CHNi, 1C). ³¹P{¹H} NMR (C₆D₆): 70.5.

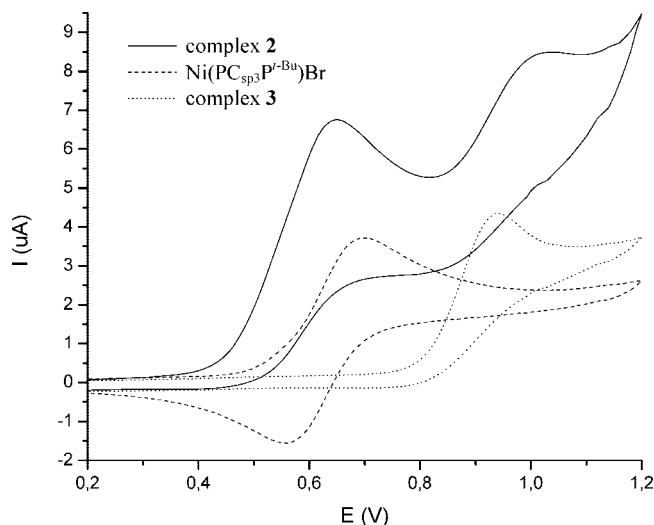


Figure 5. Cyclic voltammograms of complexes **2**, **3**, and $\text{Ni}(\text{PC}_{\text{sp}^3}\text{P}^{i\text{-Bu}})\text{Br}$ in CH_2Cl_2 (1 mM solutions) measured at 298 K with 0.1 M of TBAH as electrolyte (scan rate 100 mV s^{-1}).

observation strongly suggests that, contrary to the commonly proposed mechanism for Ni-catalyzed Kumada coupling reactions,²² the coupling reaction catalyzed by **2** does not involve any Ni^0 intermediate because formation of Ni^0 species by reductive elimination from **4** would deplete the concentration of this compound irreversibly.²³

The observation of small amounts of the homocoupling product biphenyl in the coupling reaction can signal the involvement of an electron transfer process.²⁴ We have also considered the alternative possibility that the reaction of the *in situ* generated Ni–Me derivative with PhCl might produce MeCl and a Ni–Ph intermediate instead of the anticipated products PhMe and the Ni–Cl complex; the Ni–Ph derivative could then react with PhCl to produce Ph–Ph and regenerate the Ni–Cl species. We found, however, that refluxing mixtures of the independently prepared Ni–Ph derivative **6** (0.01 M) and 100 equiv of PhCl in THF for 20 h did not give any biphenyl or Ni–Cl complex, thus ruling out the involvement of a Ni–Ph intermediate in the formation of biphenyl. Studies are underway to glean more information about the mechanism of this reaction.

Oxidation of 2. In order to assess the extent of electron donation from the various ligands to the nickel center, we subjected the PCP compounds **2**, $(\text{PC}_{\text{sp}^3}\text{P}^{i\text{-Bu}})\text{NiBr}$, and **3** to electrochemical experiments. The results of cyclic voltammetry measurements (Figure 5) indicate that the ease of $\text{Ni}^{\text{II}} \rightarrow \text{Ni}^{\text{III}}$ oxidation²⁵ follows the order **2** > $(\text{PC}_{\text{sp}^3}\text{P}^{i\text{-Bu}})\text{NiBr}$ > **3**, which

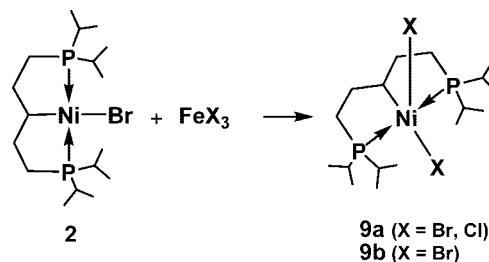
(22) Collman, J. P.; Hegedus, L. S.; Norton, J. R.; Finke, R. G. *Principles and Application of Organotransition Metal Chemistry*; University Science Books: Mill Valley, CA, 1987.

(23) To be sure, a putative Ni^0 intermediate can oxidatively add PhCl and give rise to a new Ni^{II} species that might participate in the catalytic process. However, this newly formed Ni^{II} compound would not exhibit the same spectral pattern as **4**. Therefore, observation of the ^{31}P signal for **4** as the only signal during the course of the catalysis and in the final reaction mixture suggests that the only P-bearing species involved in the coupling reaction are $(\text{PCP})\text{NiX}$ ($\text{X} = \text{Cl}, \text{Me}$).

(24) A radical mechanism involving an electron transfer from the Ni^{II} center to ArX , followed by formation of X^- and Ar^\cdot radicals, is often proposed for the observation of homocoupling products. See for instance: Tsou, T. T.; Kochi, J. K. *J. Am. Chem. Soc.* **1979**, *101*, 7547.

(25) It should be noted that a differential pulse voltammetry experiment performed under the same conditions on ferrocene and complex **2** has established that the latter shows a similar redox behavior to ferrocene in terms of one-electron redox process: $W_{1/2}(\text{ferrocene}) \sim 185 \text{ mV}$; $W_{1/2}(\text{complex } \mathbf{2}) \sim 170 \text{ mV}$.

Scheme 6



is consistent with the greater net donation of electron density by $\text{PC}_{\text{sp}^3}\text{P}$ versus $\text{PC}_{\text{sp}^2}\text{P}$ and $\text{PC}_{\text{sp}^3}\text{P}^{i\text{-Pr}}$ versus $\text{PC}_{\text{sp}^3}\text{P}^{i\text{-Bu}}$ ligands. It is particularly noteworthy that the most electron-rich compound, **2**, appears to be undergoing a second oxidation step, presumably generating a Ni^{IV} species.²⁶

The ease of oxidation of **2** prompted us to attempt its chemical oxidation and isolation of high-valent species. We did not succeed in generating Ni^{IV} species, but reaction of **2** with FeX_3 ($\text{X} = \text{Cl}, \text{Br}$) formed reddish species identified by X-ray crystallography as the trivalent complexes $(\text{PC}_{\text{sp}^3}\text{P}^{i\text{-Pr}})\text{NiX}_2$, **9** (Scheme 6). The solid state structure of complex **9a** ($\text{X} = \text{Cl}$) could not be determined accurately due to a complex disorder present in its crystalline structure,²⁷ but the structure of **9b** ($\text{X} = \text{Br}$) was resolved successfully; the ORTEP view for **9b** is shown in Figure 6, and the crystal data and collection details are listed in Table 1. This paramagnetic 17-electron species adopts a distorted square-pyramidal geometry wherein the nickel center is displaced out from the $\text{P}(1)\text{--C}(3)\text{--P}(2)\text{--Br}(1)$ plane toward the $\text{Br}(2)$ atom by 0.354 \AA .²⁸ There was only a very slight deviation from a square-pyramidal geometry of **2**, as reflected in the small value of the τ parameter for this complex (0.03);²⁹ a similarly negligible trigonal distortion was found in the analogous Ni^{III} complex $(\text{POC}_{\text{sp}^3}\text{OP}^{i\text{-Pr}})\text{NiBr}_2$ ($\tau = 0.05$).^{10a}

Conclusion

A combination of crystallographic and reactivity studies as well as electrochemical measurements have revealed interesting differences in the structures, electronic properties, and reactivities of PCP pincer complexes of nickel. Both the phosphorus substituents of the PCP ligand and the hybridization of the cyclometalated carbon atom have significant influence on the chemistry of these complexes. For instance, the $\text{PC}_{\text{sp}^3}\text{P}^{i\text{-Pr}}$ ligand stabilizes the Ni–Bu derivative toward β -H elimination; in contrast, the Ni–Bu derivative is unstable with the $\text{PC}_{\text{sp}^3}\text{P}^{i\text{-Bu}}$ system under the same conditions.³⁰ Similarly, $(\text{PC}_{\text{sp}^3}\text{P}^{i\text{-Pr}})\text{NiBr}$ was found to be a better catalyst than its $\text{PC}_{\text{sp}^2}\text{P}^{i\text{-Pr}}$ and $\text{PC}_{\text{sp}^3}\text{P}^{i\text{-Bu}}$ analogues for Kumada coupling; studies are underway to determine the scope of this and other coupling reactions.

The electrochemical measurements have hinted that Ni^{III} and Ni^{IV} species can be generated *in situ*. Although the isolation of a stable Ni^{IV} species was not achieved, the preparation of a trivalent Ni complex has been possible, and future efforts will

(26) One of the reviewers of our manuscript has invoked the possibility that the second oxidation step is due to a Ni^{III} species featuring an unpaired electron stabilized on the pincer ligand. This scenario seems less realistic to us because we believe that the aliphatic skeleton of the $\text{PC}_{\text{sp}^3}\text{P}$ ligand should not be suited to stabilizing an unpaired electron, but this alternative explanation cannot be ruled out.

(27) We believe that the disorder found in single crystals obtained from this compound arises from the presence of a mixture of Cl and Br atoms in the coordination sphere of Ni^{III} .

(28) The corresponding value for the second independent molecule of the asymmetric unit was found to be 0.331 \AA .

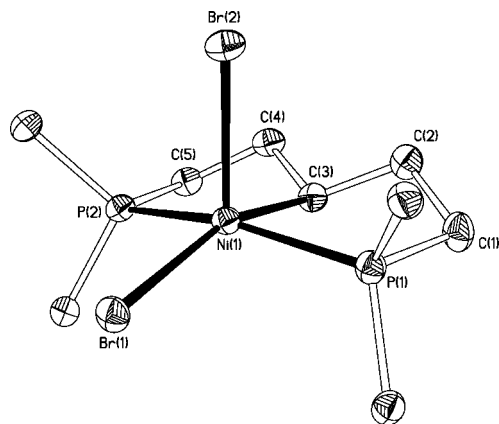


Figure 6. ORTEP diagram for one of the two molecules in the asymmetric unit of complex **9b**. Thermal ellipsoids are shown at the 30% probability level. Hydrogens and methyl carbons of the *i*-Pr groups are omitted for clarity. Selected bond distances (Å) and angles (deg) for the molecule shown: Ni(1)–C(3) = 2.039(3), Ni(1)–P(1) = 2.2719(10), Ni(1)–P(2) = 2.2762(10), Ni(1)–Br(1) = 2.4144(6), Ni(1)–Br(2) = 2.4735(7), C(3)–Ni(1)–Br(1) = 159.41(10), C(3)–Ni(1)–Br(2) = 95.96(10), P(1)–Ni(1)–P(2) = 161.11(4), P(1)–Ni(1)–Br(1) = 93.88(3), P(1)–Ni(1)–Br(2) = 95.42(3), P(2)–Ni(1)–Br(1) = 93.71(3), P(2)–Ni(1)–Br(2) = 99.35(3), P(1)–Ni(1)–C(3) = 83.37(10), P(2)–Ni(1)–C(3) = 83.46(10).

be directed toward finding new pincer ligands that can allow the isolation of high-valent Ni complexes.

Experimental Section

General Comments. All manipulations were carried out under a nitrogen atmosphere using standard Schlenk techniques and/or in a nitrogen-filled glovebox, except where noted. Solvents were purified by distillation from appropriate drying agents before use. All reagents were used as received from commercial vendors. LiC≡CPh was synthesized from the reaction of HC≡CPh with *n*-BuLi. All the NMR spectra were recorded at ambient temperature on Bruker instruments: AV400 (^1H , $^1\text{H}\{^3\text{P}\}$, $^3\text{P}\{^1\text{H}\}$) and ARX400 ($^{13}\text{C}\{^1\text{H}\}$). The ^1H and ^{13}C NMR spectra were referenced to solvent resonances, as follows: 7.26 and 77.16 ppm for CHCl_3 and CDCl_3 , respectively, and 7.15 and 128.06 ppm for $\text{C}_6\text{D}_5\text{H}$ and C_6D_6 , respectively. Assignments were confirmed by DEPT135, COSY, and HMQC experiments. The $^3\text{P}\{^1\text{H}\}$ NMR spectra were referenced to an external 85% H_3PO_4 sample (0 ppm). The IR spectra were recorded on a Perkin-Elmer 1750 FTIR (4000–450 cm^{-1}) with samples prepared as KBr pellets. The GC/MS analyses were done using a Agilent Technologies 6890 Network GC system equipped with a HP-5MS capillary column and a 5973 MS selective detector. The $^{\nu}J$ term used refers to the apparent coupling constant of the virtual triplets. The elemental analyses were performed by the Laboratoire d'Analyse Élémentaire (Université de Montréal).

***i*-Pr₂P(CH₂)₅P(*i*-Pr)₂.** A procedure for the preparation of this ligand has been published elsewhere,³¹ but we describe here a more

detailed and higher-yielding protocol.³² Lithium wire (8.000 g, 1152.57 mmol) was washed with hexanes right before use to remove the mineral oil in which it is stored, cut into thin pieces, and quickly added to a solution of chlorodiisopropylphosphine (8.0 mL, 50.27 mmol) in THF (80 mL). This mixture was cooled immediately with an ice bath and then allowed to warm slowly to room temperature. After 16 h, the mixture was cooled again to 0 °C and 1,5-dibromopentane (3.43 mL, 25.18 mmol) was added dropwise. The solvent was evaporated after 1 h, hexanes (80 mL) were added with stirring, and the resulting mixture was filtered. The filtrate was washed with degassed water and evaporated to give the desired ligand as an oil (6.657 g, 87%), which was used without further purification. ^1H NMR (CDCl_3): 0.82 (dd, $^3J_{\text{HH}} = 7.2$ Hz, $^3J_{\text{PH}} = 9.7$ Hz, $\text{CH}(\text{CH}_3)_2$, 12 H), 0.85 (dd, $^3J_{\text{HH}} = 7.2$ Hz, $^3J_{\text{PH}} = 13.6$ Hz, $\text{CH}(\text{CH}_3)_2$, 12 H), 1.11 (m, CH_2P , 4H), 1.25 (m, $\text{CH}_2\text{CH}_2\text{CH}_2\text{P}$, 6H), 1.47 (m, $\text{CH}(\text{CH}_3)_2$, 4H). $^{13}\text{C}\{^1\text{H}\}$ NMR (CDCl_3): 18.69 (d, $^2J_{\text{PC}} = 9.7$ Hz, $\text{CH}(\text{CH}_3)_2$, 4C), 20.00 (d, $^2J_{\text{PC}} = 15.2$ Hz, $\text{CH}(\text{CH}_3)_2$, 4C), 21.33 (d, $^1J_{\text{PC}} = 16.5$ Hz, CH_2P , 2C), 23.13 (d, $^1J_{\text{PC}} = 11.7$ Hz, $\text{CH}(\text{CH}_3)_2$, 4C), 27.83 (d, $^2J_{\text{PC}} = 17.9$ Hz, $\text{CH}_2\text{CH}_2\text{P}$, 2C), 33.30 (t, $^3J_{\text{PC}} = 11.4$ Hz, $\text{CH}_2\text{CH}_2\text{CH}_2\text{P}$, 1C). $^3\text{P}\{^1\text{H}\}$ NMR (CDCl_3): 3.9 (s). ^1H NMR (C_6D_6): 1.01 (dd, $^3J_{\text{HH}} = 6.9$ Hz, $^3J_{\text{PH}} = 10.4$ Hz, $\text{CH}(\text{CH}_3)_2$, 12 H), 1.05 (dd, $^3J_{\text{HH}} = 7.0$ Hz, $^3J_{\text{PH}} = 13.3$ Hz, $\text{CH}(\text{CH}_3)_2$, 12 H), 1.30 (m, CH_2P , 4H), 1.45–1.65 ($\text{CH}_2\text{CH}_2\text{CH}_2\text{P}$ and $\text{CH}(\text{CH}_3)_2$, 10H). $^{13}\text{C}\{^1\text{H}\}$ NMR (C_6D_6): 19.08 (d, $^2J_{\text{PC}} = 10.3$ Hz, $\text{CH}(\text{CH}_3)_2$, 4C), 20.42 (d, $^2J_{\text{PC}} = 16.5$ Hz, $\text{CH}(\text{CH}_3)_2$, 4C), 22.20 (d, $^1J_{\text{PC}} = 19.3$ Hz, CH_2P , 2C), 23.80 (d, $^1J_{\text{PC}} = 13.8$ Hz, $\text{CH}(\text{CH}_3)_2$, 4C), 28.55 (d, $^2J_{\text{PC}} = 19.3$ Hz, $\text{CH}_2\text{CH}_2\text{P}$, 2C), 33.81 (t, $^3J_{\text{PC}} = 11.7$ Hz, $\text{CH}_2\text{CH}_2\text{CH}_2\text{P}$, 1C). $^3\text{P}\{^1\text{H}\}$ NMR (C_6D_6): 2.9 (s).

***i*-Pr₂PCH₂C₆H₄CH₂P(*i*-Pr)₂.** A synthesis of this ligand has already been published elsewhere,³³ but we describe here a higher-yielding and faster protocol. Lithium wire (6.000 g, 864.43 mmol) was washed with hexanes right before use to remove the mineral oil in which it is stored, cut into thin pieces, and quickly added to a solution of chlorodiisopropylphosphine (6.0 mL, 37.70 mmol) in THF (60 mL). This mixture was cooled immediately with an ice bath and then allowed to warm slowly to room temperature. After 16 h, the mixture was cooled again to 0 °C, and a solution of α,α' -dichloro-*m*-xylene (3.300 g, 18.85 mmol) in THF (20 mL) was added dropwise. The solvent was evaporated after 1 h, hexanes (100 mL) were added with stirring, and the resulting mixture was filtered. The filtrate was washed with degassed water and evaporated to give the desired ligand as an oil (4.280 g, 67%), which was used without further purification. For NMR details, see ref 33.

{*i*-Pr₂P(CH₂)₅P(*i*-Pr)₂]₂NiBr₄ (1). *i*-Pr₂P(CH₂)₅P(*i*-Pr)₂ (0.200 g, 0.66 mmol) was added to a suspension of anhydrous NiBr₂ (0.144 g, 0.66 mmol) in toluene (10 mL), and the mixture was heated to 80 °C for 2 h. The solvent was then removed under reduced pressure to give complex **1** as a dark purple solid (0.320 g, 93%). ^1H NMR (CDCl_3): 1.39 (d, $^3J_{\text{HH}} = 7.0$ Hz, $\text{CH}(\text{CH}_3)_2$, 24H), 1.64 (d, $^3J_{\text{HH}} = 7.2$ Hz, $\text{CH}(\text{CH}_3)_2$, 24H), 1.35–1.95 ($\text{CH}_2\text{CH}_2\text{CH}_2\text{P}$, 20H), 2.47 (m, $\text{CH}(\text{CH}_3)_2$, 8H). $^{13}\text{C}\{^1\text{H}\}$ NMR (CDCl_3): 18.81 (s, $\text{CH}(\text{CH}_3)_2$, 8C), 20.20 (s, CH_2P , 4C), 20.54 (s, $\text{CH}(\text{CH}_3)_2$, 8C), 24.69 (s, $\text{CH}(\text{CH}_3)_2$, 8C), 26.50 (s, $\text{CH}_2\text{CH}_2\text{P}$, 4C), 35.03 (s, $\text{CH}_2\text{CH}_2\text{CH}_2\text{P}$, 2C). Anal. Calcd for $\text{C}_{34}\text{H}_{76}\text{Br}_4\text{P}_4\text{Ni}_2$: C, 39.05; H, 7.32. Found: C, 38.74; H, 7.54.

{*i*-Pr₂PCH₂(CH₂)₂CH]₂NiBr (2). *i*-Pr₂P(CH₂)₅P(*i*-Pr)₂ (2.000 g, 6.57 mmol) was added to a suspension of anhydrous NiBr₂ (1.722 g, 7.88 mmol) and DMAP (0.803 g, 6.57 mmol) in toluene (40 mL), and the reaction mixture was refluxed for 12 h. The solvent was then evaporated to dryness, hexanes (40 mL) were added, and the resultant mixture was filtered in the air on a glass frit. The filtrate was washed with water and concentrated until a minimum

(29) The τ parameter is calculated according to the relationship $\tau = (\beta - \alpha)/60$, wherein α and β refer to the largest basal angles in the complex ($\beta > \alpha$); values approaching zero imply small degrees of deviation from an ideal square-pyramidal geometry, whereas values approaching 1 signal significant distortions toward a trigonal bipyramidal geometry: Addison, A. W.; Rao, T. N.; Reedijk, J.; van Rijn, J.; Verschoor, G. C. *J. Chem. Soc., Dalton Trans.* **1984**, 1349.

(30) For other examples of Ni-alkyl complexes that are resistant to β -H elimination see: (a) Liang, L.-C.; Lin, J.-M.; Hung, C.-H. *Organometallics* **2003**, *22*, 3007. (b) Stollenz, M.; Rudolph, M.; Görls, H.; Walther, D. *J. Organomet. Chem.* **2003**, *687*, 153.

(31) Geier, S.; Goddard, R.; Holle, S.; Jolly, P. W.; Krüger, C.; Lutz, F. *Organometallics* **1997**, *16*, 1612.

(32) The yield of ligand remains unchanged whether the synthesis is done under an argon or nitrogen atmosphere.

(33) Rytbchinski, B.; Ben-David, Y.; Milstein, D. *Organometallics* **1997**, *16*, 3786.

of hexanes was left. Golden-brown crystals of **2** formed by keeping the solution at $-14\text{ }^{\circ}\text{C}$ for 1 h (1.065 g, 37%). ^1H NMR (C_6D_6): 0.97 (dvt, $^3J_{\text{HH}} \sim ^\nu J_{\text{PH}} = 5.8\text{--}6.6\text{ Hz}$, $\text{CH}(\text{CH}_3)_2$, 6H), 1.13 (dvt, $^3J_{\text{HH}} \sim ^\nu J_{\text{PH}} = 6.6\text{--}6.8\text{ Hz}$, $\text{CH}(\text{CH}_3)_2$, 6H), 1.46 (dvt, $^3J_{\text{HH}} \sim ^\nu J_{\text{PH}} = 7.5\text{--}7.7\text{ Hz}$, $\text{CH}(\text{CH}_3)_2$, 12H), 1.00–1.70 ($\text{CH}_2\text{CH}_2\text{P}$, 8H), 1.78 (m, CHNi , 1H), 2.06–2.24 ($\text{CH}(\text{CH}_3)_2$, 4H). $^1\text{H}\{^3\text{P}\}$ NMR (C_6D_6): 0.97 (d, $^3J_{\text{HH}} = 7.1\text{ Hz}$, $\text{CH}(\text{CH}_3)_2$, 6H), 1.13 (d, $^3J_{\text{HH}} = 7.0\text{ Hz}$, $\text{CH}(\text{CH}_3)_2$, 6H), 1.46 (d, $^3J_{\text{HH}} = 7.1\text{ Hz}$, $\text{CH}(\text{CH}_3)_2$, 12H). $^{13}\text{C}\{^1\text{H}\}$ NMR (C_6D_6): 17.56 (s, $\text{CH}(\text{CH}_3)_2$, 2C), 18.61 (s, $\text{CH}(\text{CH}_3)_2$, 2C), 19.36 (vt, $^\nu J_{\text{PC}} = 2.8\text{ Hz}$, $\text{CH}(\text{CH}_3)_2$, 2C), 19.94 (vt, $^\nu J_{\text{PC}} = 1.7\text{ Hz}$, $\text{CH}(\text{CH}_3)_2$, 2C), 22.12 (vt, $^\nu J_{\text{PC}} = 10.3\text{ Hz}$, CH_2P , 2C), 23.38 (vt, $^\nu J_{\text{PC}} = 10.7\text{ Hz}$, $\text{CH}(\text{CH}_3)_2$, 2C), 25.46 (vt, $^\nu J_{\text{PC}} = 9.7\text{ Hz}$, $\text{CH}(\text{CH}_3)_2$, 2C), 38.94 (vt, $^\nu J_{\text{PC}} = 10.3\text{ Hz}$, $\text{CH}_2\text{CH}_2\text{P}$, 2C), 52.30 (t, $^2J_{\text{PC}} = 9.0\text{ Hz}$, CHNi , 1C). $^{31}\text{P}\{^1\text{H}\}$ NMR (C_6D_6): 67.4. Anal. Calcd for $\text{C}_{17}\text{H}_{37}\text{BrNiP}_2$: C, 46.19; H, 8.44. Found: C, 45.97; H, 8.83.

{(i-Pr)₂PCH₂(CH₂)₂CH}NiBr (3). The preparation of this complex from $\text{Ni}(\text{cod})_2$ and the corresponding brominated ligand has already been reported;^{6g} we report here another synthetic pathway. *i*-Pr₂PCH₂-C₆H₄CH₂P(*i*-Pr)₂ (0.500 g, 1.48 mmol) was added to a solution of anhydrous NiBr_2 (0.387 g, 1.77 mmol) and DMAP (0.180 g, 1.48 mmol) in ethanol (10 mL), and the reaction mixture was refluxed for 1.5 h. The solvent was then evaporated to dryness, the Schlenk was opened to air, and hexanes (40 mL) were added. The resultant mixture was filtered in the air on a glass frit and the filtrate evaporated to give complex **3** as a yellow solid (0.281 g, 40%). ^1H NMR (CDCl_3): 1.17 (dvt, $^3J_{\text{HH}} \sim ^\nu J_{\text{PH}} = 6.7\text{--}7.0\text{ Hz}$, $\text{CH}(\text{CH}_3)_2$, 12H), 1.45 (dvt, $^3J_{\text{HH}} \sim ^\nu J_{\text{PH}} = 7.4\text{--}8.4\text{ Hz}$, $\text{CH}(\text{CH}_3)_2$, 12H), 2.38 (m, $\text{CH}(\text{CH}_3)_2$, 4H), 3.08 (vt, $^\nu J_{\text{PH}} = 3.7\text{ Hz}$, PCH_2 , 4H), 6.91 (s, *ArH*, 3H). $^{13}\text{C}\{^1\text{H}\}$ NMR (CDCl_3): 18.31 (s, $\text{PCH}(\text{CH}_3)_2$, 4C), 19.12 (s, $\text{PCH}(\text{CH}_3)_2$, 4C), 24.01 (vt, $^\nu J_{\text{PC}} = 11.0\text{ Hz}$, $\text{PCH}(\text{CH}_3)_2$, 4C), 32.83 (vt, $^\nu J_{\text{PC}} = 12.8\text{ Hz}$, PCH_2 , 2C), 122.26 (vt, $^\nu J_{\text{PC}} = 9.0\text{ Hz}$, *ArH*, 2C), 125.35 (s, *ArH*, 1C), 152.46 (t, $J_{\text{PC}} = 13.1\text{ Hz}$, *ArCH}_2, 2C), 159.13 (t, $^2J_{\text{PC}} = 15.9\text{ Hz}$, *Ar*_{ipso}, 1C). $^{31}\text{P}\{^1\text{H}\}$ NMR (CDCl_3): 61.8 (s). Anal. Calcd for $\text{C}_{20}\text{H}_{35}\text{BrNiP}_2$: C, 50.46; H, 7.41. Found: C, 49.94; H, 7.53.*

{(i-Pr)₂PCH₂(CH₂)₂CH}NiMe (4). MeMgCl (0.15 mL of a 3 M solution in THF, 0.45 mmol) was added to a solution of **2** (0.200 g, 0.45 mmol) in toluene (2.5 mL). After 5 min, the solvents were evaporated, hexanes (20 mL) were added, and the resultant suspension was filtered. The filtrate was washed with degassed water (3 × 20 mL) and evaporated to dryness to give complex **4** as a yellow powder (0.121 g, 71%). ^1H NMR (C_6D_6): -0.50 (t, $^3J_{\text{PH}} = 7.7\text{ Hz}$, NiCH_3 , 3H), 0.96 (dvt, $^3J_{\text{HH}} \sim ^\nu J_{\text{PH}} = 5.5\text{--}6.3\text{ Hz}$, $\text{CH}(\text{CH}_3)_2$, 6H), 1.12 (dvt, $^3J_{\text{HH}} \sim ^\nu J_{\text{PH}} = 6.2\text{--}6.5\text{ Hz}$, $\text{CH}(\text{CH}_3)_2$, 6H), 1.21 (m, $\text{CH}(\text{CH}_3)_2$, 12H), 0.80–2.20 ($\text{CH}(\text{CH}_3)_2$, $\text{CH}_2\text{CH}_2\text{P}$, CHNi , 13H). $^{13}\text{C}\{^1\text{H}\}$ NMR (C_6D_6): -18.64 (t, $^2J_{\text{PC}} = 19.9\text{ Hz}$, NiCH_3 , 1C), 17.55 (s, $\text{CH}(\text{CH}_3)_2$, 2C), 19.01 (s, $\text{CH}(\text{CH}_3)_2$, 2C), 19.46 (vt, $^\nu J_{\text{PC}} = 3.3\text{ Hz}$, $\text{CH}(\text{CH}_3)_2$, 2C), 19.63 (vt, $^\nu J_{\text{PC}} = 2.4\text{ Hz}$, $\text{CH}(\text{CH}_3)_2$, 2C), 22.68 (vt, $^\nu J_{\text{PC}} = 9.5\text{ Hz}$, $\text{CH}(\text{CH}_3)_2$, 2C), 25.81 (vt, $^\nu J_{\text{PC}} = 10.4\text{ Hz}$, CH_2P , 2C), 25.85 (vt, $^\nu J_{\text{PC}} = 9.0\text{ Hz}$, $\text{CH}(\text{CH}_3)_2$, 2C), 37.70 (vt, $^\nu J_{\text{PC}} = 10.9\text{ Hz}$, $\text{CH}_2\text{CH}_2\text{P}$, 2C), 58.56 (t, $^2J_{\text{PC}} = 9.5\text{ Hz}$, CHNi , 1C). $^{31}\text{P}\{^1\text{H}\}$ NMR (C_6D_6): 71.4. Anal. Calcd for $\text{C}_{18}\text{H}_{40}\text{NiP}_2 \cdot \text{H}_2\text{O}$: C, 54.71; H, 10.71. Found: C, 54.39; H, 10.48.

{(i-Pr)₂PCH₂(CH₂)₂CH}NiC≡CMe (5). To complex **2** (1.000 g, 2.26 mmol) was added $\text{MeC}\equiv\text{CMgBr}$ (4.52 mL of a 0.5 M solution in THF, 2.26 mmol) and the mixture stirred. After 5 min, the solvent was evaporated, hexanes (40 mL) were added, and the resultant suspension was filtered. The filtrate was washed with degassed water (3 × 20 mL) and the solvent evaporated to dryness to give complex **5** as a yellow powder (0.716 g, 79%). ^1H NMR (C_6D_6): 1.02 (m, $\text{CH}(\text{CH}_3)_2$, 6H), 1.14 (m, $\text{CH}(\text{CH}_3)_2$, 6H), 1.25–1.50 (m, $\text{CH}(\text{CH}_3)_2$, 12H), 0.80–2.20 ($\text{CH}(\text{CH}_3)_2$, $\text{CH}_2\text{CH}_2\text{P}$, CHNi , 13H), 2.13 (s, $\text{C}\equiv\text{CCH}_3$, 3H). $^{13}\text{C}\{^1\text{H}\}$ NMR (C_6D_6): 7.61 (s, $\text{C}\equiv\text{CCH}_3$, 1C), 17.81 (s, $\text{CH}(\text{CH}_3)_2$, 2C), 18.74 (s, $\text{CH}(\text{CH}_3)_2$, 2C), 19.40 (vt, $^\nu J_{\text{PC}} = 2.5\text{ Hz}$, $\text{CH}(\text{CH}_3)_2$, 2C), 19.68 (s, $\text{CH}(\text{CH}_3)_2$, 2C), 23.93 (vt, $^\nu J_{\text{PC}} = 11.1\text{ Hz}$, $\text{CH}(\text{CH}_3)_2$, 2C), 24.76 (vt, $^\nu J_{\text{PC}} = 9.6\text{ Hz}$, CH_2P , 2C),

25.90 (vt, $^\nu J_{\text{PC}} = 10.6\text{ Hz}$, $\text{CH}(\text{CH}_3)_2$, 2C), 38.41 (vt, $^\nu J_{\text{PC}} = 10.6\text{ Hz}$, $\text{CH}_2\text{CH}_2\text{P}$, 2C), 56.38 (t, $^2J_{\text{PC}} = 10.1\text{ Hz}$, CHNi , 1C), 98.44 (t, $^2J_{\text{PC}} = 30.8\text{ Hz}$, $\text{C}\equiv\text{CCH}_3$, 1C) 115.74 (s, $\text{C}\equiv\text{CCH}_3$, 1C). $^{31}\text{P}\{^1\text{H}\}$ NMR (C_6D_6): 76.1. $^{31}\text{P}\{^1\text{H}\}$ NMR (CDCl_3): 76.0. IR (KBr): 2100 cm^{-1} ($\mu_{\text{C}\equiv\text{C}}$). Anal. Calcd for $\text{C}_{20}\text{H}_{40}\text{NiP}_2$: C, 59.88; H, 10.05. Found: C, 60.12; H, 10.33.

{(i-Pr)₂PCH₂(CH₂)₂CH}NiPh (6). PhMgBr (0.90 mL of a 1 M solution in THF, 0.90 mmol) was added to a solution of **2** (0.400 g, 0.90 mmol) in toluene (5.0 mL), and the mixture was stirred and refluxed for 1 h. The solvent was then evaporated, hexanes (20 mL) were added, and the resultant suspension was filtered. The filtrate was washed with degassed water (3 × 20 mL) and evaporated to dryness to give complex **6** as a yellow-brown powder (0.245 g, 62%). ^1H NMR (C_6D_6): 0.87–1.05 (m, $\text{CH}(\text{CH}_3)_2$, 24H), 0.85–2.50 ($\text{CH}(\text{CH}_3)_2$, $\text{CH}_2\text{CH}_2\text{P}$, CHNi , 13H), 6.90–7.80 (Ph, 5H). $^{13}\text{C}\{^1\text{H}\}$ NMR (C_6D_6): 17.64 (s, $\text{CH}(\text{CH}_3)_2$, 2C), 17.79 (s, $\text{CH}(\text{CH}_3)_2$, 2C), 18.53 (s, $\text{CH}(\text{CH}_3)_2$, 2C), 18.97 (s, $\text{CH}(\text{CH}_3)_2$, 2C), 22.84 (vt, $^\nu J_{\text{PC}} = 10.7\text{ Hz}$, $\text{CH}(\text{CH}_3)_2$, 2C), 24.44 (vt, $^\nu J_{\text{PC}} = 10.1\text{ Hz}$, $\text{CH}(\text{CH}_3)_2$, 2C), 25.84 (vt, $^\nu J_{\text{PC}} = 10.7\text{ Hz}$, CH_2P , 2C), 37.98 (vt, $^\nu J_{\text{PC}} = 10.7\text{ Hz}$, $\text{CH}_2\text{CH}_2\text{P}$, 2C), 56.81 (t, $^2J_{\text{PC}} = 8.9\text{ Hz}$, CHNi , 1C), 120.78 (s, *Ph*, 1C), 125.80 (s, *Ph*, 1C), 127.49 (s, *Ph*, 1C), 129.06 (s, *Ph*, 1C), 140.55 (s, *Ph*, 1C), 168.77 (t, $^2J_{\text{PC}} = 24.0\text{ Hz}$, *Ph* (C_{ipso}), 1C). $^{31}\text{P}\{^1\text{H}\}$ NMR (C_6D_6): 68.1. Anal. Calcd for $\text{C}_{23}\text{H}_{42}\text{NiP}_2 \cdot \text{H}_2\text{O}$: C, 60.42; H, 9.70. Found: C, 60.89; H, 9.73.

{(i-Pr)₂PCH₂(CH₂)₂CH}NiBu (7). Addition of *n*-BuLi (52 μL of a 2.5 M solution in hexanes, 0.131 mmol) to a concentrated solution of **2** (0.058 g, 0.131 mmol) in benzene-*d*₆ (0.6 mL) resulted in the instantaneous formation of the butyl species **7**, as observed by NMR spectroscopy. ^1H NMR (C_6D_6): 0.50 (m, $\text{CH}_2(\text{CH}_2)_2\text{CH}_3$, 2H). $^{13}\text{C}\{^1\text{H}\}$ NMR (C_6D_6): 0.51 (t, $^2J_{\text{PC}} = 19.0\text{ Hz}$, $\text{CH}_2(\text{CH}_2)_2\text{CH}_3$, 1C), 14.46 (s, $\text{CH}_2(\text{CH}_2)_2\text{CH}_3$, 1C), 17.91 (s, $\text{CH}(\text{CH}_3)_2$, 2C), 18.74 (s, $\text{CH}(\text{CH}_3)_2$, 2C), 19.52 (vt, $^\nu J_{\text{PC}} = 3.4\text{ Hz}$, $\text{CH}(\text{CH}_3)_2$, 2C), 20.00 (vt, $^\nu J_{\text{PC}} = 2.7\text{ Hz}$, $\text{CH}(\text{CH}_3)_2$, 2C), 23.74 (vt, $^\nu J_{\text{PC}} = 9.5\text{ Hz}$, $\text{CH}(\text{CH}_3)_2$, 2C), 25.90 (vt, $^\nu J_{\text{PC}} = 11.4\text{ Hz}$, CH_2P , 2C), 25.94 (vt, $^\nu J_{\text{PC}} = 8.3\text{ Hz}$, $\text{CH}(\text{CH}_3)_2$, 2C), 31.02 (s, $\text{CH}_2(\text{CH}_2)_2\text{CH}_3$, 1C), 36.41 (t, $^3J_{\text{PC}} = 2.3\text{ Hz}$, $\text{CH}_2(\text{CH}_2)_2\text{CH}_3$, 1C), 37.45 (vt, $^\nu J_{\text{PC}} = 10.2\text{ Hz}$, $\text{CH}_2\text{CH}_2\text{P}$, 2C), 57.50 (t, $^2J_{\text{PC}} = 9.5\text{ Hz}$, CHNi , 1C). $^{31}\text{P}\{^1\text{H}\}$ NMR (C_6D_6): 68.1.

{(i-Pr)₂PCH₂(CH₂)₂CH}NiC≡CPh (8). **Method A.** Reaction of complex **4** (0.021 g, 0.06 mmol) with $\text{HC}\equiv\text{CPh}$ (6 μL , 0.06 mmol) in DMSO-*d*₆ (0.8 mL) for 15 h led to full conversion of the starting material into complex **8**, as observed by NMR spectroscopy. **Method B.** Refluxing a mixture of complex **5** (0.020 g, 0.05 mmol) and excess $\text{HC}\equiv\text{CPh}$ (100 μL , 0.91 mmol) in toluene (0.8 mL) for 2 h led to the full conversion of the starting material into the phenylacetylide complex **8**, as observed by $^{31}\text{P}\{^1\text{H}\}$ NMR spectroscopy. **Method C.** Reacting $\text{LiC}\equiv\text{CPh}$ (0.110 g, 1.02 mmol) with complex **2** (0.300 g, 0.679 mmol) in toluene (3 mL) at room temperature for 1 h gave complex **8**, as observed by $^{31}\text{P}\{^1\text{H}\}$ NMR spectroscopy. $^{13}\text{C}\{^1\text{H}\}$ NMR (CDCl_3): 17.87 (s, $\text{CH}(\text{CH}_3)_2$, 2C), 18.72 (s, $\text{CH}(\text{CH}_3)_2$, 2C), 19.36 (s, $\text{CH}(\text{CH}_3)_2$, 2C), 19.67 (s, $\text{CH}(\text{CH}_3)_2$, 2C), 23.84 (vt, $^\nu J_{\text{PC}} = 11.4\text{ Hz}$, $\text{CH}(\text{CH}_3)_2$, 2C), 24.31 (vt, $^\nu J_{\text{PC}} = 9.9\text{ Hz}$, CH_2P , 2C), 25.79 (vt, $^\nu J_{\text{PC}} = 10.4\text{ Hz}$, $\text{CH}(\text{CH}_3)_2$, 2C), 37.89 (vt, $^\nu J_{\text{PC}} = 10.3\text{ Hz}$, $\text{CH}_2\text{CH}_2\text{P}$, 2C), 57.35 (t, $^2J_{\text{PC}} = 9.4\text{ Hz}$, CHNi , 1C), 120.12 (t, $^2J_{\text{PC}} = 29.0\text{ Hz}$, $\text{C}\equiv\text{CPh}$, 1C), 122.29 (s, 1C), 123.71 (s, *Ph*, 1C), 127.79 (s, *Ph*, 2C), 130.06 (s, 1C), 130.34 (s, *Ph*, 2C). $^{31}\text{P}\{^1\text{H}\}$ NMR (CDCl_3): 77.9.

{(i-Pr)₂PCH₂(CH₂)₂CH}NiX₂ (9). To a solution of **2** (0.100 g, 0.23 mmol) in CH_2Cl_2 (10 mL) was added FeCl_3 (0.037 g, 0.23 mmol) or FeBr_3 (0.067 g, 0.23 mmol). The mixture was stirred 5 min and filtered through a glass frit. Complex **9a** was obtained quantitatively as a red powder after evaporation of the filtrate to dryness. ^1H NMR (C_6D_6): 0.5–3.0 (broad resonances). The combustion data are consistent with either $\text{Ni}(\text{PC}_{\text{sp}^3}\text{P}^{\text{i-Pr}})\text{ClBr}$ or an equimolar mixture of $\text{Ni}(\text{PC}_{\text{sp}^3}\text{P}^{\text{i-Pr}})\text{Br}_2$ and $\text{Ni}(\text{PC}_{\text{sp}^3}\text{P}^{\text{i-Pr}})\text{Cl}_2$. Anal. Calcd for $\text{C}_{17}\text{H}_{37}\text{BrNiClP}_2$: C, 42.76; H, 7.81. Found: C, 42.96; H, 7.21. Complex **9b** could not be purified due to similar

solubility properties to FeBr₂; single crystals used in the X-ray diffraction studies were obtained by recrystallizing a small batch from the slow evaporation of a CH₂Cl₂ solution of the complex.

General Procedure for Kumada Coupling. MeMgCl (0.98 mL of a 3.0 M solution in THF, 2.94 mmol) was added to a solution of PhCl (200 μ L, 1.97 mmol), *p*-xylene (60 μ L, 0.49 mmol, used as an internal standard), and the catalyst in THF (1.0 mL). The mixture was heated to reflux for the desired time. A sample of the reaction was then withdrawn, diluted with diethyl ether, and washed with water. The organic phase was dried over MgSO₄ and filtered, and the resultant solution was analyzed by GC/MS.

Crystal Structure Determinations. Single crystals of these complexes were grown from slow diffusion of hexanes into a saturated solution of the complex in benzene-*d*₆ (**1**) or slow evaporation of a dichloromethane solution (**9b**) or hexanes solutions at -15 °C (**2**, **4**, **6**) or at room temperature (**3** and **5**). The crystallographic data (Table 1) for complexes **1**, **3**, and **5** were collected on a Bruker CCD 2k diffractometer (sealed tube) using graphite monochromatic Cu K α radiation, equipped with a 3 circle platform goniometer and a Bruker Smart 2000 area detector. The crystallographic data for complexes **2**, **4**, **6**, and **9b** were collected on a Nonius FR591 generator (rotating anode) equipped with a Montel 200, a D8 goniometer, and a Bruker Smart 6000 area detector.

Cell refinement and data reduction were done using SAINT.³⁴ An empirical absorption correction, based on the multiple measurements of equivalent reflections, was applied using the program SADABS.³⁵ The space group was confirmed by XPREP routine³⁶ in the program SHELXTL.³⁷ The structures were solved by direct methods and refined by full-matrix least-squares and difference Fourier techniques with SHELX-97.³⁸ All non-hydrogen atoms were refined with anisotropic displacement parameters. Hydrogen atoms

were set in calculated positions and refined as riding atoms with a common thermal parameter. For complex **3**, the possible presence of ethanol molecules in the structure (237 electrons corresponding to 9 molecules per unit cell) has been determined using the program PLATON,³⁹ but no correction of the data has been applied.

Cyclic Voltammetry Experiments. Cyclic voltammetry measurements were performed using a BAS Epsilon potentiostat. A typical three-electrode system was used, consisting of a Pt working electrode, a Pt auxiliary electrode, and a Ag/AgCl reference electrode ($E_{1/2}(\text{FeCp}_2^+/\text{FeCp}_2) = +0.63$ V under these conditions). The experiments were carried out in CH₂Cl₂ at room temperature with TBAH as electrolyte (0.1 M), and the solutions were bubbled with nitrogen before each experiment.

Complete details of the X-ray analyses for complexes **1–6** and **9b** have been deposited at the Cambridge Crystallographic Data Centre (CCDC 631839 (**1**), 631840 (**2**), 671730 (**3**), 631841 (**4**), 631843 (**5**), 631842 (**6**), 689350 (**9b**)). These data can be obtained free of charge via www.ccdc.cam.ac.uk/data_request/cif, or by e-mailing data_request@ccdc.cam.ac.uk, or by contacting the Cambridge Crystallographic Data Centre, 12 Union Road, Cambridge CB2 1EZ, UK; fax: +44 1223 336033.

Acknowledgment. The authors are grateful to Dr. Dominic Rochefort for helpful discussions and also for his assistance with the electrochemical measurements, to Mr. Denis Spasyuk for his preliminary work on the Kumada coupling system, to Université de Montréal for fellowships to A.C., and to NSERC of Canada for financial support of this work.

Supporting Information Available: X-ray analyses for complexes **1–6** and **9b**. This material is available free of charge via the Internet at <http://pubs.acs.org>.

OM8005454

(34) SAINT Release 6.06, Integration Software for Single Crystal Data; Bruker AXS Inc.: Madison, WI, 1999.

(35) Sheldrick, G. M. SADABS, Bruker Area Detector Absorption Corrections; Bruker AXS Inc.: Madison, WI, 1999.

(36) XPREP Release 5.10, X-ray data Preparation and Reciprocal Space Exploration Program; Bruker AXS Inc.: Madison, WI, 1997.

(37) SHELXTL Release 5.10, The Complete Software Package for Single Crystal Structure Determination; Bruker AXS Inc.: Madison, WI, 1997.

(38) (a) Sheldrick, G. M. SHELXS97, Program for the Solution of Crystal Structures; Univ. of Gottingen: Germany, 1997. (b) Sheldrick, G. M. SHELXL97, Program for the Refinement of Crystal Structures; University of Gottingen: Germany, 1997.

(39) Spek, A. L. PLATON, Molecular Geometry Program; University of Utrecht: Holland, 2002.